ACTA STEREOL 1987; 6/SUPPL II: 87–100
ISS COMMEMORATIVE-MEMORIAL VOLUME
ORIGINAL SCIENTIFIC PAPER

THREE-DIMENSIONAL ANALYSIS OF THE SPATIAL DISTRIBUTION OF PARTICLES USING THE TANDEM-SCANNING REFLECTED LIGHT MICROSCOPE

A. J. Baddeley *

C. V. Howard †

A. Boyde **

S. Reid **

* CSIRO Division of Mathematics and Statistics
P.O. Box 218, Lindfield, N.S.W., 2070, Australia.

† Department of Anatomy, University of Liverpool,
PO Box 147, Liverpool L69 3BX, U.K.

** Department of Anatomy and Embryology, University College London, London
WC1E 6BT, U.K.

SUMMARY

Osteocyte lacunae in whole mineralised bone were observed directly without sectioning, using the TSRLM. Inside a sampling region the three-dimensional coordinates of the centre points of the lacunae were recorded. Preliminary statistical analysis is reported here. Evidence of systematic packing of lacunae was found. Biological variability was considerable for N_V but negligible for the spatial interaction function K.

KEYWORDS: Biological variation, K function, particle density, ratio estimation, sampling, spatial interaction, spatial statistics, stereology.

1 INTRODUCTION

A full understanding of the spatial relationship between particles in a three-dimensional structure can only be achieved by collecting three-dimensional coordinate information. The cost of collecting such data has always been considered prohibitive using standard histological technique. By contrast, the mapping of 2-dimensional coordinates of particle profiles in sections is commonplace. Statistical methods for analysing 2-dimensional point patterns are well-developed (Ripley (1977), Diggle (1981)) and have been applied in microscopy by Appleyard *et al.* (1985) and Pedro *et al.* (1984). It is worth noting that the statistical theory extends, with few modifications, to 3 and higher dimensions.

Petran *et al.* (1968) described the tandem-scanning reflected light microscope (TSRLM) which permits the non-destructive observation of internal structures in whole tissue by taking thin *optical* sections at the focal plane of the objective lens. This plane may be moved up and down through the tissue, to sample a complete three-dimensional volume. The application of this microscope in examining whole bone and tooth specimens has been described by Boyde *et al.* (1982). The numerical density N_V of osteocyte lacunae in whole bone has been measured directly on the TSRLM by Howard *et al.* (1985) using an unbiased 3-dimensional counting rule analogous to the 2-dimensional Gundersen tiling rule.

In this paper we present a method for the unbiased collection of 3-dimensional coordinate data for the locations of any particles which can be visualised in the TSRLM. The method is demonstrated on osteocyte lacunae in primate monkey skulls. A statistical technique for analysing such data is presented and demonstrated on the primate data. Tentative conclusions are drawn about the spatial distribution of osteocyte lacunae. The results also provide information about the inter- and intra-animal variability in N_V and $K(r)$ estimates.

2 DATA COLLECTION

The parietal bones of three fully articulated adult Macaque monkey (*Macaca fascicularis*) skulls from the collection of University College London were used. The right parietal bone was examined, in each case, approximately 1 cm lateral to the sagittal suture and 2 cm posterior to the coronal suture. The skulls were mounted on plasticine on a moving stage placed beneath the TSRLM. Immersion oil was applied and a $\times 60$, NA 1.0 oil immersion objective lens (Lomo) was focussed at 10 μm below the cranial surface. The TV image was produced by a Panasonic WB 1850/B camera on a Sony PVM 90CE TV monitor.

A graduated rectangular counting frame 90 × 110 mm (representing 82 × 100 μm in real units) was marked on a Perspex overlay and fixed to the screen. The area of tissue seen within the frame defined a subfield: a guard area of 10 mm width was visible on all sides of the frame. Ten subfields were examined, arranged approximately in a rectangular grid pattern, with at least one field width separating each pair of fields. The initial field position was determined randomly by applying a randomly-generated coordinate shift to the moving stage. Subsequent fields were attained using the coarse controls of the microscope stage, in accordance with the rectangular grid pattern.

For each subfield, the focal plane was racked down from its initial 10 μm depth until all visible osteocyte lacunae had been examined. This depth d was recorded. The 3-dimensional sampling volume was therefore a rectangular box of dimensions 82 × 100 × d microns, called a "brick". For each visible lacuna, the fine focus racking control was adjusted until maximum brightness was obtained. The depth of the focal plane was then recorded as the z coordinate of the "centre point" of the lacuna. Without moving the focal plane, the x and y coordinates of the centre of the lacunar image were read off the graduated counting frame. This required a subjective judgement of the position of the centre of the 2-dimensional image. Profiles were approximately elliptical and the centre was considered to be well-defined. Accuracy of the recording procedure was tested by independent repetition (by the same operator and by different operators) and found to be reproducible to ±2 mm on the screen.

A lacuna was counted only if its (x, y) coordinates lay inside the 90 × 110mm counting frame. The (x, y, z) coordinates were manually recorded and later entered into a mainframe computer for analysis.

3 STATISTICAL METHOD

3.1 Background

Techniques for the analysis of 2-dimensional point patterns are described by Ripley (1981) and Diggle (1983). A popular method is based on the *K-function* which describes the interaction between pairs of points in the pattern (see, e.g. Diggle, 1983, 46-49 and 70-89). Given a point pattern, we arbitrarily choose one of the points in the pattern as a reference point. For each radius $r > 0$ we define $K(r)$ to be the mean number of points in the pattern that lie within a radius r of the chosen point, divided by the mean number of points per unit area N_A:

$$K(r) = \frac{E(\text{number of points within distance } r \text{ of an arbitrary point})}{N_A} \quad (1)$$

where E denotes expected value (i.e. mean) taken over all possible outcomes of the random pattern. This definition applies to any stationary (statistically homogeneous) random point process. A 3-dimensional version of the K function is exactly analogous:

$$K(r) = \frac{E(\text{number of points within distance } r \text{ of an arbitrary point})}{N_V} \quad (2)$$

where as usual N_V is the expected number of points per unit volume.

Thus $K(r)$ is a measure of how many points are expected to be found within r units of a typical point in the pattern. It is a theoretical characteristic based on a 'population average' over all possible outcomes of the random point pattern. In this sense it can be compared to the stereological population averages V_V, S_V etc. Methods for estimating $K(r)$ from data are discussed in the next subsection.

Interpretation of $K(r)$ in 3 dimensions is similar to the 2-dimensional case outlined by Ripley and by Diggle. If the pattern is completely random in the sense that points in different sub-regions are statistically independent (the *Poisson* pattern) then the mean number of points inside a sphere of radius r is simply N_V times the volume of the sphere, so we have

$$K(r) = \frac{4}{3}\pi r^3$$

for a Poisson pattern. Alternatively, if points tend to cluster or "attract" each other, then typically $K(r) > \frac{4}{3}\pi r^3$ for values of r corresponding to the range of attraction. If the points "repel" one another or are systematically spaced, typically $K(r) < \frac{4}{3}\pi r^3$ for some values of r. In this way the K function constitutes a simple and easily-interpreted summary of the pattern.

It should be noted that the K function, along with alternative measures of spatial interaction described in Chapter 5 of Diggle (1983), is only a summary statistic and should not be read as a *characterisation* of the point pattern. For example, two quite different point patterns may have the same K function (Baddeley & Silverman, 1984). This insensitivity is a feature of most current techniques in spatial statistics. Analysis of a point pattern should normally include several

alternative measures of interaction. In the present report, for brevity and because of some special features of the data, we shall use only the K function.

3.2 Estimation

The quantities N_A, N_V, $K(r)$ are theoretical averages over all possible outcomes of a hypothetical random point process. A set of data from a real, observed point pattern should be regarded as just one single outcome of a random point process. On the basis of such data, we can only *estimate* the true K function. The estimator of $K(r)$ based on the data is denoted by $\hat{K}(r)$.

Let the sampling region (in which the points were observed) be denoted by B. Number the points in some arbitrary fashion $1, 2, \ldots, n$ and let d_{ij} be the distance between points i and j. In 2 dimensions, the usual estimator of $K(r)$ is

$$\hat{K}(r) = \frac{\text{area}(B)}{n^2} \sum_{d_{ij} \leq r} w_{ij}^{-1} \tag{3}$$

where w_{ij} is an "edge-correction factor" equal to the proportion of the circumference of the circle with centre at point i and radius d_{ij} which lies within the sampling window B. See, e.g. Diggle (1983, p. 71). For each fixed r, $\hat{K}(r)$ is an approximately unbiased estimator of the true $K(r)$ of the random point pattern. The bias increases with r. Ripley and Diggle generally recommend the estimate of $K(r)$ should only be employed for $r < D/4$ where D is the minimum diameter of the sampling window B.

In 3 dimensions, the analogous estimator of $K(r)$ is

$$\hat{K}(r) = \frac{\text{volume}(B)}{n^2} \sum_{d_{ij} \leq r} w_{ij}^{-1} \tag{4}$$

where w_{ij} is now the proportion of the *surface area* of the *sphere* with centre at point i and radius d_{ij} which lies within the sampling volume B.

In stereological terms, $\hat{K}(r)$ in (3)-(4) is a ratio estimator. First consider the estimation of N_V. The usual estimator is

$$\hat{N_V} = \frac{n}{\text{volume}(B)} \tag{5}$$

where n is the number of points observed in the sampling region B. This is the best (i.e. minimum variance) unbiased estimator of N_V. Define

$$Y(r) = (N_V)^2 K(r) \tag{6}$$

This is the expected number of ordered *pairs* of points that are less than r units apart, with the first point lying in a unit volume. Moment theory of stationary processes (e.g. Stoyan and Mecke (1983), p.55) shows that

$$\hat{Y}(r) = \frac{1}{\text{volume}(B)} \sum_{d_{ij} \le r} w_{ij}^{-1} \tag{7}$$

is an **unbiased** estimator of $Y(r)$ for any stationary 3-dimensional point process. The sum is over pairs of points lying in the sampling window B. Again this is the best (minimum variance) unbiased estimator. Comparing (4) with (7) shows that

$$\hat{K}(r) = \frac{\hat{Y}(r)}{(\hat{N}_V)^2} \tag{8}$$

is the ratio of an unbiased estimator to the square of another unbiased estimator.

3.3 Stereological aspects

Typically the methods presented by Ripley (1977) and Diggle (1981) for 2-dimensional point patterns assume that the data consist of a *single* point pattern observed in a defined region. Indeed, this causes theoretical difficulties, because the data are not independently repeatable in the usual way, and a direct estimate of the variability of estimators (2), (4) is unavailable.

Stereological sampling is quite different. Usually the sampling is (conceptually) repeatable, and the data contain replicated observations (e.g. sufficiently large numbers of plane sections, tissue blocks and experimental animals). Miles (1978) explains the importance of proper specification of the stereological sampling regime and of any assumptions made about the experimental material. The importance of replication at various levels of the experiment, and of quantifying the variability at each level, is stressed by Gundersen & Østerby (1981).

Suppose we are able to observe a 3-dimensional point pattern inside several sampling windows $B_1, \ldots, B_m$ and the windows are far enough apart to be regarded

as independent observations. We could estimate $K(t)$ by the pooled average

$$\hat{K}_{ave}(r) = \frac{1}{m}\sum_{l=1}^{m}\hat{K}_l(r) \tag{9}$$

where $\hat{K}_l(r)$ represents the estimator in equation (4) derived from the point pattern observed in window B_l for $l = 1,\ldots,m$.

The standard deviation of this estimator is approximately $1/\sqrt{m}$ times the standard deviation of $\hat{K}_l(r)$. The latter can be estimated from the data by the usual formula for the sample standard deviation. Note that $\hat{K}_{ave}(r)$ has the same bias as each of the individual estimators $\hat{K}_l(r)$, i.e. $\hat{K}_{ave}(r)$ is an approximately unbiased estimator of $K(r)$ for small r, but the bias does *not* decrease with the number m of samples.

The simple average (9) is justifiable if the sampling volumes B_l are of equal size, and if there are no other data relevant to the estimation of K. Otherwise, it may be more appropriate to use a weighted average. Cruz Orive (1980) showed that ratio estimation methods (Cochran (1977)) typically produce more accurate estimates of stereological parameters such as V_V that can be expressed as ratios of aggregate quantities. Recalling (8) we propose the ratio estimator for $K(r)$,

$$\hat{K}_{quad}(r) = \frac{\sum_{l=1}^{m}\hat{Y}_l(r)}{\sum_{l=1}^{m}\hat{N}_{V(l)}^{\,2}} \tag{10}$$

where $\hat{Y}_l(r)$ and $\hat{N}_{V(l)}$ denote the estimates obtained from sampling region B_l for $l = 1,\ldots,m$. Thus $\hat{K}_{quad}$ is a ratio of averages, whereas $\hat{K}_{ave}$ is an average of ratios. Alternatively using (8) we can recognise (10) as a weighted average of the individual estimates:

$$\hat{K}_{quad}(r) = \frac{\sum_{l=1}^{m} a_l\hat{K}_l(r)}{\sum_{l=1}^{m} a_l} \tag{11}$$

where $a_l = \hat{N}_{V(l)}^{\,2}$.

The bias and standard deviation of the ratio estimator $\hat{K}_{quad}$ are known theoretically up to an approximation (Cochran (1977), p. 117; Cruz Orive (1980)) and can be estimated from the data:

$$\mathrm{Var}\left(\hat{K}_{quad}(r)\right) \approx \frac{1}{m} K(r)^2 \{C_{xx} + C_{yy} - 2C_{xy}\} \tag{12}$$

and for the bias

$$\mathbf{E}\left(\hat{K}_{quad}(r) - K(r)\right) \approx \frac{1}{m} \{K(r)C_{xx} - C_{xy}\} \tag{13}$$

where C_{xx}, C_{xy}, C_{yy} are the entries in the relative covariance matrix of $(\hat{Y}(r), \hat{N_V}^2)$. The bias is approximately proportional to $1/m$, i.e. bias decreases with the number of sampling windows (Cochran (1977), p. 117). This is important, because it allows us to estimate $K(r)$ for values of r larger than the recommended maximum distance $D/4$ discussed in paragraph 3.2.

The standard deviation of the ratio estimator is approximately proportional to $1/\sqrt{m}$, as for the naive estimator. The choice between $\hat{K}_{ave}$ and $\hat{K}_{quad}$ depends on how well a scatter plot of the estimates $(\hat{Y}(r), \hat{N_V}^2)$ fits a straight line through the origin, as measured by standard least-squares regression. If the fit is good then according to (12), $\hat{K}_{quad}$ will be more accurate (less biased and smaller variance) than $\hat{K}_{ave}$. We would generally expect the ratio estimator to be better.

The typical stereological sampling experiment is a nested sampling design in which several individuals (e.g. animals) are each sampled within several 3-dimensional blocks (e.g. tissue blocks) which are in turn each sectioned several times. Analysis-of-variance techniques can be used to quantify the variability at each level of the experiment (Gundersen & Østerby, 1981). These procedures will be adopted in the present experiment because we have 3 animals each providing 10 sampling regions or bricks for analysis.

4 ANALYSIS

First we report on the estimation of N_V. Table 1 shows the individual estimates $\hat{N_V}$ for each brick. The means for each animal are 23.6, 36.3, 34.8 (lacunae $/10^6$ cubic microns) for animals Z4, Z5, Z9 respectively, with standard error 1.7. The overall mean is 31.6 with standard error 4.1.

Animal	N_V estimates									
Z4	35.7	22.6	24.7	24.7	20.3	16.5	20.8	28.5	22.2	19.8
Z5	30.2	41.2	37.0	38.4	37.0	27.2	49.4	37.0	30.4	35.0
Z9	37.0	32.3	29.2	28.2	38.2	35.8	40.1	32.9	33.4	41.2

Table 1: Estimates of N_V (number per 10^6 cubic microns)

An analysis of variance is in Table 2. This is a standard one-way analysis based on a variance components model, i.e. assuming constant inter-brick variance across animals. There is some suggestion that animal Z9 has a lower variation between bricks, but we set this aside in the present preliminary report. The variation in numerical density N_V between animals is estimated at about 22% CV (i.e. standard deviation as a fraction of the grand mean). The variation in estimates of N_V between bricks is put at 17% CV.

The effect of taking 10 bricks per animal is that the estimate of N_V for each animal has about 5% CE (coefficient of error, i.e. standard error of the estimate divided by the mean), while the effect of taking 3 animals with 10 bricks per animal is that the overall estimate of average N_V has about 13% CE. For the purposes of estimating average N_V it would have been more efficient to take fewer bricks and more animals. This reinforces the claims in Gundersen & Østerby (1981) that biological variation tends to overshadow other sources of variation in stereological nested sampling.

Next we have calculated individual estimates of $K(r)$ for each brick in each animal, according to equation (4). The estimates for each brick in animal Z4 are presented in Figure 1 and compared with the theoretical Poisson K-function. There is a remarkable degree of coherence between the individual graphs, considering that each brick contained only 20 to 40 points.

SOURCE	df	SS	MS	SD	CV
animals	2	967.1	483.5	6.95	22%
bricks	27	790.1	29.3	5.41	17%
total	29	1757.2			

Table 2: Analysis of variance for Table 1

Figure 1. Estimates of K for each brick in animal Z4 (solid lines) compared with the theoretical Poisson curve (dotted)

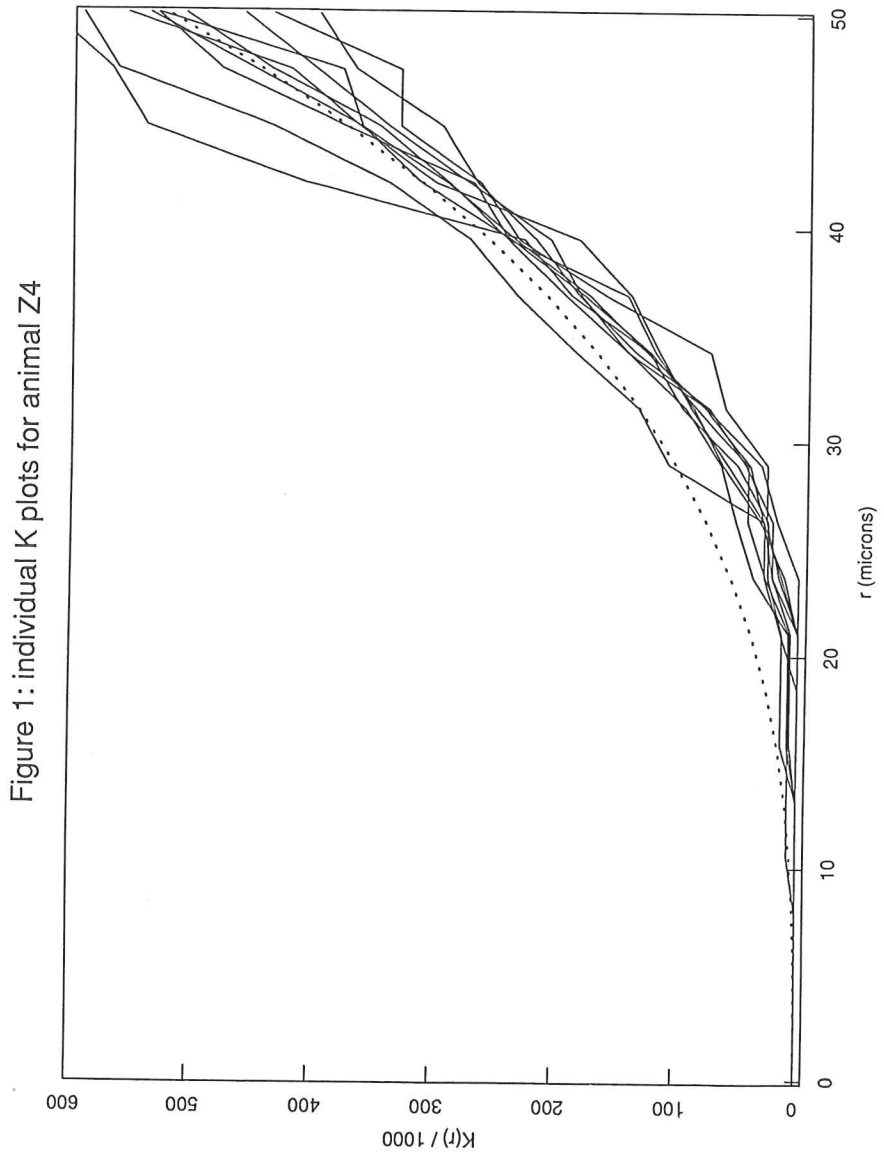

Figure 2. Scatter plot of estimates of Y against estimates of NV (numbers 4, 5, 9 refer to animals Z4, Z5, Z9)

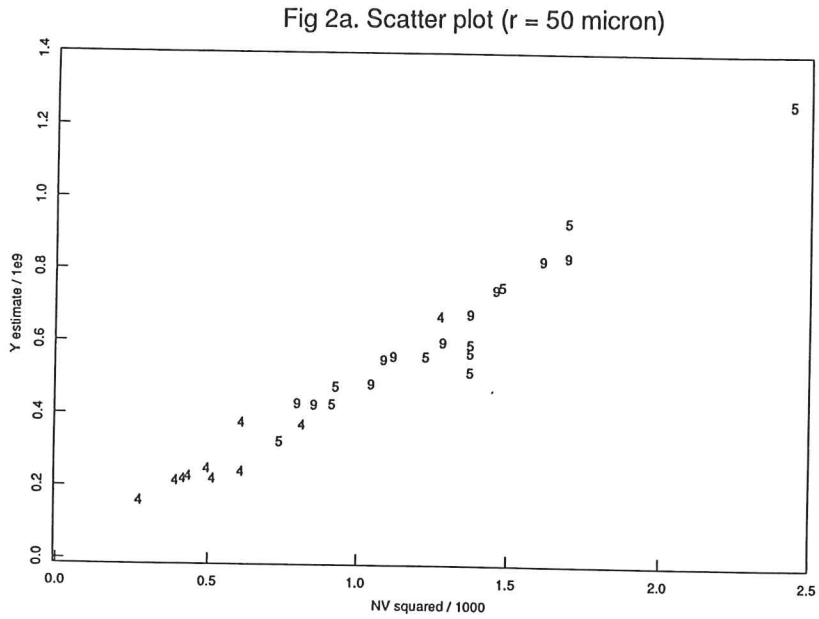

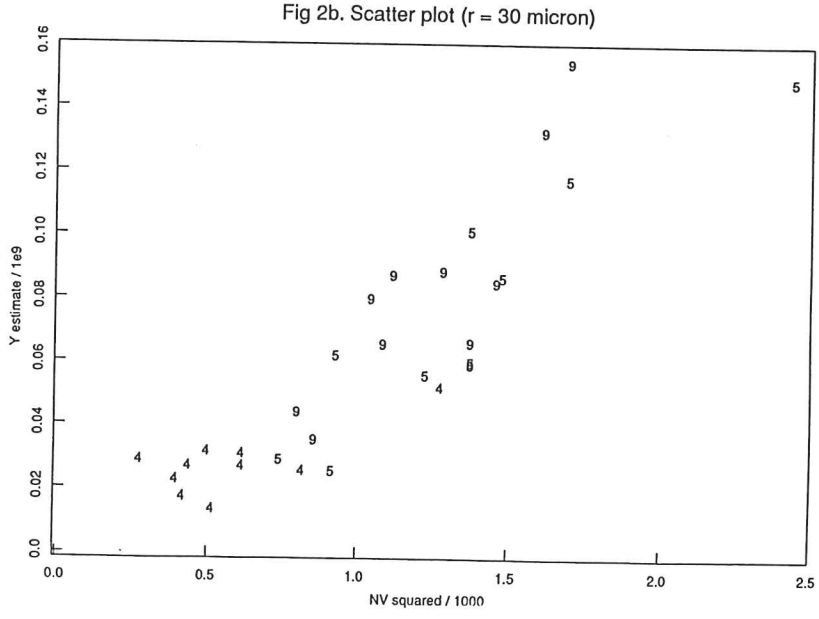

Figure 3. Estimates of K obtained by ratio regression (solid lines) with pointwise confidence limits (dashed) and Poisson curve (dotted)

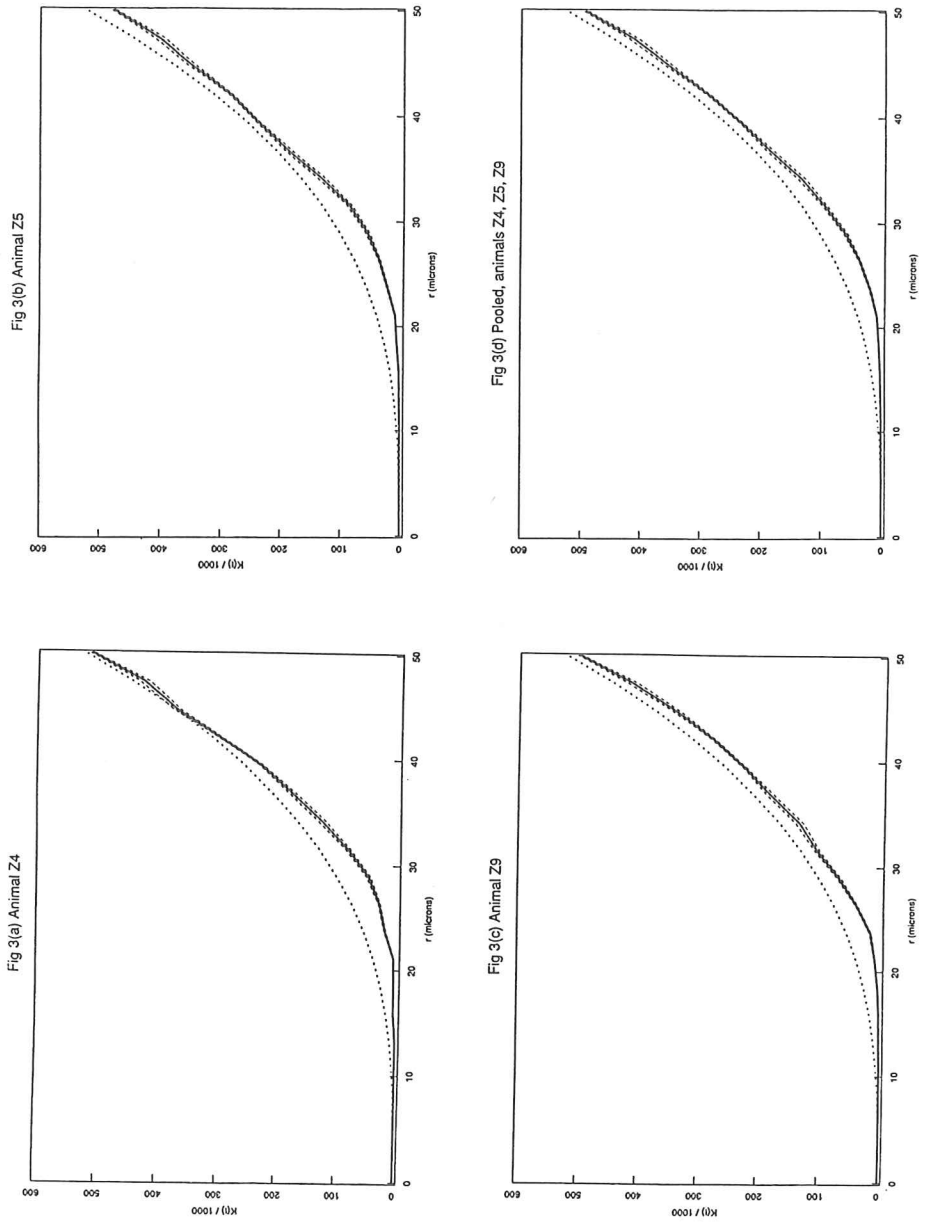

To check the validity of the ratio estimator (10), we plotted the estimates of $Y(r)$ against the corresponding $(\hat{N}_V)^2$ for each brick, with r fixed. The plots are Figures 2 (a) and (b) for $r = 50$ and $r = 30$ microns respectively, with labels 4, 5, 9 corresponding to the animals Z4, Z5, Z9. The regression model holds very well.

Finally in Figure 3 we exhibit ratio estimates $\hat{K}_{quad}(r)$ for the K function of each animal, and a pooled $\hat{K}_{quad}(r)$ estimate. The confidence limits for each fixed r form the 95% confidence interval based on the t-distribution and using the estimate of standard deviation derived from ratio estimation, equation (12). Thus the confidence limits are strictly only to be applied for a fixed r. Nevertheless, they can be taken as a confidence band (simultaneously over all r) with somewhat lower significance level.

The deviation from the Poisson K is clearly identified. The estimates show a pronounced dip in the K function in the range 15–35 microns, suggesting a regular or inhibitory pattern of points.

The differences between the estimated K functions for the three animals are surprisingly small. This may suggest that, while cell density N_V is subject to biological variability, spatial interactions between osteocytes in developing bone are invariant and therefore probably under strict genetical control. This in turn makes us wonder how significant a quantity N_V is in biological research. It is possible that cellular spatial relationships will prove to be more sensitive indices of structure and function.

REFERENCES

1. Appleyard, S. T., Witkowski, J. A., Ripley, B. D., Shotton, D. M. and Dubowitz, V.
A novel procedure for pattern analysis of features present on freeze-fractured plasma membranes. *J. Cell Sci.* **74** (1985) 105-117.

2. Baddeley, A. J. and Silverman, B. W.
A cautionary example on the use of second-order methods for analyzing point patterns. *Biometrics* **40** (1984) 1089-1093.

3. Boyde, A., Petran, M. and Hadravsky, M.
Tandem scanning reflected light microscopy of internal features in whole bone and tooth samples. *J. Microsc.* **132** (1982) 1-7.

4. Cochran, W. G.
Sampling Techniques. 3rd ed. 1977. New York: John Wiley and Sons.

5. Cruz Orive, L.-M.
Best linear unbiased estimators for stereology. *Biometrics* **36** (1980) 595-605.

6. Diggle, P. J.
Statistical analysis of spatial point patterns. New York: Academic Press 1983.

7. Gundersen, H. J. G. and Østerby, R.
Optimizing sampling efficiency of stereological studies in biology: or 'Do more less well!' *J. Microscopy* **121** (1981) 65-73.

8. Howard, V., Reid, S., Baddeley, A. and Boyde, A.
Unbiased estimation of particle density in the tandem scanning reflected light microscope. *J. Microsc.* **138** (1985) 203-212.

9. Miles, R. E.
The importance of proper model specification in stereology. In *Geometrical Probability and Biological Structures: Buffon's 200th Anniversary.* Proceedings, Paris 1977. R.E. Miles and J. Serra (eds.) 115-136. Lecture Notes in Biomathematics no. 23. Berlin: Springer-Verlag 1978.

10. Pedro, N., Carmo-Fonseca, M. and Fernandes, P.
Quantitative analysis of pore patterns on rat prostate nuclei using spatial statistics methods. *J. Microsc.* **134** (1984) 271-280.

11. Petran, M., Hadravsky, M., Egger, M.D. and Galambos, R.
Tandem-scanning reflected light microscope. *J. Opt. Soc. Amer.* **58** (1968) 661-664.

12. Ripley, B. D.
Spatial Statistics. New York: John Wiley and Sons, 1981.

13. Stoyan, D. and Mecke, J.
Stochastische Geometrie. Wissenschaftlicher Taschenbücher, Band 275. Berlin: Akademie Verlag 1983.